

# Application of ImageJ in the rock thin section image analysis: the separation and quantitative calculation of crystal-glass two phases

Ruoyu Hu<sup>a</sup>, Fuchun Li<sup>a\*</sup>, Huan Yu<sup>a</sup>, Jian Yang<sup>a</sup>

DOI: 10.25177/JESES.4.3.RA.502

Research

Received Date: 15<sup>th</sup> Apr 2019

Accepted Date: 24<sup>th</sup> Apr 2019

Published Date: 27<sup>th</sup> Apr 2019

Copy rights: © This is an Open access article distributed under the terms of International License.



<sup>a</sup>College of Resources and Environmental Sciences, Nanjing Agricultural University, Nanjing, Jiangsu 210095, China

## CORRESPONDENCE AUTHOR

Fuchun Li

Email: fchli@njau.edu.cn

## CITATION

Ruoyu Hu, Fuchun Li, Huan Yu, Jian Yang, Application of ImageJ in the rock thin section image analysis: the separation and quantitative calculation of crystal-glass two phases(2019) SDRP Journal of Earth Sciences & Environmental Studies 4(3)

## ABSTRACT

We often have geometric measurement, quantitative calculation and other requirements for the electronic images, formed by digital polarizing microscope or scanning electron microscope and so on. The specific image analysis method relies on their supporting accessories and software; some of them are limited or expensive. ImageJ, a free application and designed with an open architecture, can solve almost any image processing or analysis problem, widely used in biological science, material science, medicine, and aviation. We tried to apply the ImageJ to image analysis of the rock sample, starting from the separation and quantitative calculation of the crystal-glass two phases. We verify the reliability of this method, by two groups' proportion-known samples, the mixture of potassium feldspar and glass powder glued by epikote and crystalbond509 respectively, and draw the following conclusions: (1) This method of the quantitative calculation of the crystal-glass two phases is reliable; (2) We recommend using machine recognition with a gray value around 70-80 for quantitative calculation; (3) If we want to verify this method, the selection of materials and adhesives as well as the observation conditions need to be carefully prepared. We hope the method and the ImageJ are helpful for researchers to make qualitative or quantitative judgments conveniently and there will be more extensive application space to be expected.

**Keywords:** Crystal-glass two phases; ImageJ; Image analysis; Quantitative calculation

## 1. INTRODUCTION

ImageJ is a public domain Java image processing program inspired by the National Institute of Mental Health (NIH) for the Image processing and analysis. It is widely used in biological science, material science, medicine, aviation and so on. It has a very convenient effect on image analysis of cells, metal materials and soil flakes [1,2,3]. It can calculate area and pixel value statistics of user-defined selections. It can measure distances and angles. It can create density histograms and line profile plots. ImageJ supports standard image processing functions such as contrast manipulation, sharpening, smoothing, edge detection and median filtering [4], so it can perform geometric treatment and quantitative analysis on such aspects as material micromorphological characteristics, pore structure, irregular area and microstructure. It is also important that, ImageJ was a free application and designed with an open architecture that provides extensibility via Java plugins. Custom acquisition, analysis and processing plugins can be developed using ImageJ's built in editor and Java compiler. User-written plugins make it possible to solve almost any image processing or analysis problem [5]. The above features make ImageJ a flexible and cost-effective application.

Electronic imaging analysis of rock samples always is conducted through digital polarizing microscope or scanning electron microscope. We often have geometric measurement, quantitative calculation and other requirements for the formed electronic images. Some techniques, like electron back scatter diffraction (EBSD) are very helpful to suit the requirement. [6-8], but some of the methods are limited or expensive. We note that some studies have focused on the dissolution kinetics of basaltic glasses [9], and the chemical reactions of volcanic glass of rocks in geothermal environment [10]. If the crystal-glass phases separation and quantitative calculation of complex structures can be carried out, we may have further studied on this direction. We know that mineral crystals and glasses are very different under the polarizing microscope, the field of glass under the microscope is dark as its isotropic, while the mineral crystals, as birefringent, appear as bright field at non-extinction

direction. Therefore, starting from the quantitative calculation of the crystal-glass two phases, we try to make a contribution to microstructure Image analysis, by its usage in other fields for reference.

## 2. MATERIALS AND METHODS

### 2.1 Experimental materials

Potassium feldspar granule and glass were used as verification materials in this experiment and are simulated respectively the crystalline and glassy parts of rock. We set two experiment groups respectively with epikote and crystalbond509 used as two different adhesives.

### 2.2 Experimental methods

#### 2.2.1 Samples preparation methods

Potassium feldspar and glass were crushed into 200 meshes and mixed in the following proportions: 1. glass (100%)+ potassium feldspar (0%); 2. glass (75%)+ potassium feldspar (25%); 3. glass (50%)+ potassium feldspar (50%); 4. glass (25%)+ potassium feldspar (75%); 5. glass (0%)+ potassium feldspar (100%). The five groups of materials with right proportion were fully oscillated and mixed, then were divided into two experimental groups according to numbers E1-E5 (epikote) and C1-C5 (crystalbond509), glued with epikote and crystalbond509 respectively into solids. We polished the above solids into thin section about 0.03mm for observation.

#### 2.2.2 Observation methods

We placed the prepared thin section under the polarizing microscope (Nikon eclipse 50/POL, 10 x 5) for preliminary observation, and confirmed that the view fields of the samples under the microscope are clear and homogeneous. Then, we randomly selected 10 clear view areas of each sample under the microscope to take photos, numbered them and saved. At last, we obtained 100 sample photos for analysis.

### 2.3 Analysis methods

We use imageJ (<https://imagej.nih.gov/ij/>) to process the sample figure for analysis. Operation method as follows: (1): Open the image that needs to be ana-

lyzed (2): Set the scale of the image; (3): Convert it into an 8-bit image. Now the image we opened will change as shown in figure 1; (4): Press the Image--Adjust--Threshold buttons successively in order to the image binarization. The threshold operation interface is shown in the figure 2. Drag the first slider to determine the range what we think is crystal, which will be displayed in red on the 8-bit image. The distinction is based on the difference in grayscale between the images of the two, the glass is darker than the crystal; (5): Set Measurements, check the checkbox of Area, Area fraction, Min & Max gray value, and Limit to threshold. At last, we click the "Measure" option in the label "Analyze", and get the result shown as figure 3. We record the relevant data and then repeat the operation to complete the analysis of all 100 samples.

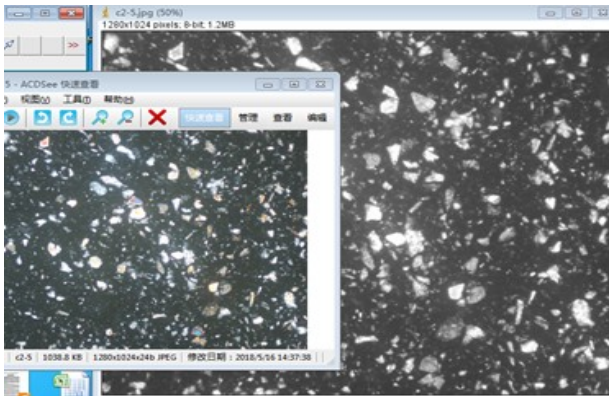


**Figure 1.** The comparison between the 8-bit image and the original.

### 3. RESULTS AND DISCUSSIONS

We found that due to some practical facts, such as light source and electron imaging, the ImageJ has different requirements on the recognition of gray level under different glass/crystal ratio. Therefore, GV (gray value) =100, GV=80, GV=75 and GV=70 were tested in group E and group C respectively, and a set of manual comparison was also conducted as the control. The result is shown as Table 1 and Table 2.

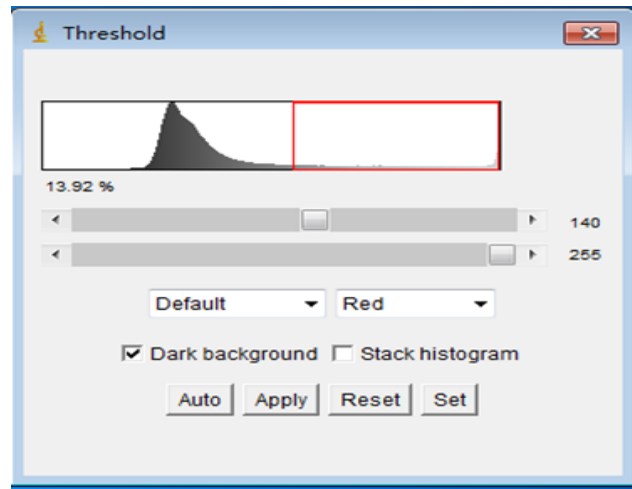


**Figure 2.** The threshold operation interface.

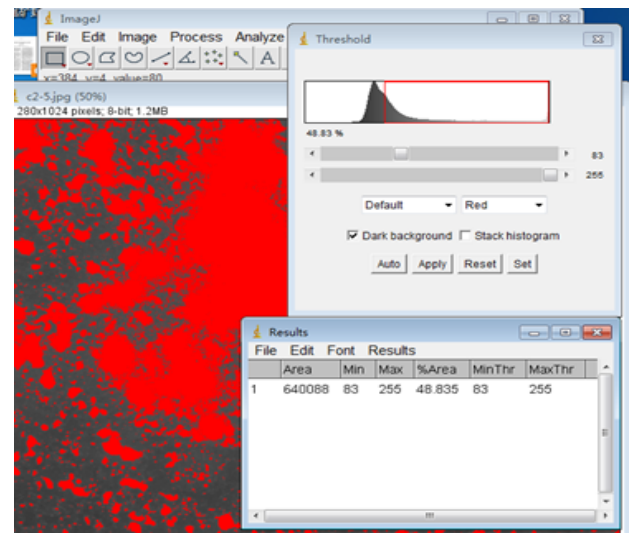


**Figure 3.** The interface of the results after been analyzed.

**Table 1.** The measured value of the crystal in group C

Number	The measured value of the machine cognition				The measured value of the manual cognition
	Gray value= 80	Gray	Gray value= 70	Gray value= 75	
C1-1	--	3.82	--	6.97	2.16(136)
C1-2	--	3.96	--	7.26	5.11(87)
C1-3	--	3.71	--	7.66	2.64(114)
C1-4	--	3.74	--	7.55	3.38(101)
C1-5	--	4.13	--	8.82	5.36(90)
C1-6	--	2.56	--	7.43	3.99(99)
C1-7	--	1.05	--	5.30	4.42(96)
C1-8	--	3.91	--	7.28	4.08(98)
C1-9	--	3.51	--	7.30	3.42(101)
C1-10	--	3.40	--	7.45	3.23(102)
AVE	--	3.38	--	7.30	3.78
C2-1	--	34.41	--	--	32.30(103)
C2-2	--	32.25	--	--	33.03(99)
C2-3	--	29.69	--	--	27.79(103)
C2-4	--	23.36	--	--	30.15(90)
C2-5	--	25.99	--	--	25.33(101)
C2-6	--	33.48	--	--	30.51(103)
C2-7	--	27.20	--	--	32.31(92)
C2-8	--	28.33	--	--	33.48(92)
C2-9	--	26.86	--	--	26.38(101)
C2-10	--	26.47	--	--	29.49(95)
AVE	--	28.80	--	--	30.07
C3-1	--	--	--	--	
C3-2	51.44	33.25	--	62.26	45.34(84)
C3-3	48.16	33.15	--	56.46	52.65(77)
C3-4	47.69	32.11	--	56.71	52.60(77)
C3-5	49.27	32.71	--	59.13	43.85(84)
C3-6	45.71	30.71	--	54.38	42.02(83)
C3-7	50.56	27.75	--	62.58	44.60(83)
C3-8	45.77	28.64	--	55.83	44.14(81)
C3-9	45.88	29.48	--	56.26	51.53(77)
C3-10	52.61	34.60	--	61.94	46.86(84)
AVE	48.57	31.38	--	58.39	47.06
C4-1	56.37	--	--	64.79	51.86(81)
C4-2	53.99	--	--	62.98	45.28(84)
C4-3	68.22	--	--	78.30	58.14(84)
C4-4	64.01	--	--	71.96	67.84(77)
C4-5	53.57	--	--	63.15	57.93(77)
C4-6	61.45	--	--	74.79	46.99(86)
C4-7	58.96	--	--	68.56	66.28(76)
C4-8	54.16	--	--	60.42	58.64(76)

C4-9	60.47	--	--	68.22	64.16(77)
C4-10	62.98	--	--	68.81	64.27(77)
AVE	59.42	--	--	68.20	58.14
C5-1	--	--	94.14	85.62	87.62(74)
C5-2	--	--	91.66	84.10	85.68(74)
C5-3	--	--	84.63	73.63	82.16(72)
C5-4	--	--	89.60	80.97	85.79(72)
C5-5	--	--	88.47	78.01	65.22(83)
C5-6	--	--	90.27	78.52	80.90(74)
C5-7	--	--	93.84	83.76	72.01(81)
C5-8	--	--	98.42	92.03	88.34(77)
C5-9	--	--	96.80	89.26	85.64(77)
C5-10	--	--	93.24	83.38	85.48(74)
AVE	--	--	92.11	82.93	81.88

Note: "--" denotes that there is a large deviation between the measured value and the theoretical value; "( )" in manual column denotes the gray value by manual

**Table 2.** The measured value of the crystal in group E

Number	The measured value of the machine cognition				The measured value of the manual cognition
	Gray value= 80	Gray value=100	Gray value=70	Gray value=75	
E1-1	5.95	3.51	9.40	7.31	3.14 (106)
E1-2	5.95	2.66	11.64	8.17	2.21 (107)
E1-3	7.26	3.21	13.56	9.69	3.56 (97)
E1-4	6.33	3.40	10.82	8.06	2.74 (110)
E1-5	5.33	2.42	10.28	7.19	2.28 (102)
E1-6	7.80	2.87	15.94	11.03	2.87 (100)
E1-7	6.01	2.26	12.64	8.65	4.96 (83)
E1-8	7.46	4.05	11.32	9.04	6.50 (84)
E1-9	7.44	3.98	11.04	8.96	5.38 (90)
E1-10	9.98	4.89	15.96	12.48	4.59 (102)
AVE	6.95	3.33	12.26	9.06	3.82
E2-1	--	32.71	--	--	17.50 (121)
E2-2	--	31.94	--	--	18.00 (118)
E2-3	--	36.78	--	--	20.56 (116)
E2-4	--	36.75	--	--	20.46 (116)
E2-5	--	34.34	--	--	19.40 (118)
E2-6	--	44.92	--	--	21.83 (114)
E2-7	--	43.83	--	--	17.64 (120)
E2-8	--	40.42	--	--	19.45 (118)
E2-9	--	32.52	--	--	22.04 (111)
E2-10	--	30.15	--	--	25.89 (104)
AVE	--	36.44	--	--	20.28
E3-1	50.58	29.40	--	--	31.67(98)
E3-2	54.68	30.36	--	--	29.35(102)

E3-3	57.52	31.73	--	--	29.11(100)
E3-4	58.09	30.96	--	--	30.75(102)
E3-5	53.80	29.93	--	--	34.37(93)
E3-6	42.71	27.90	--	--	30.35(93)
E3-7	50.78	30.39	--	--	39.89(86)
E3-8	59.40	35.17	--	--	27.18(98)
E3-9	55.02	33.09	--	--	44.27(86)
E3-10	57.70	32.18	--	--	25.61(103)
AVE	54.03	31.11	--	--	32.23
E4-1	64.70	29.61	--	--	41.24(86)
E4-2	61.00	30.93	--	--	40.06(89)
E4-3	65.16	29.11	--	--	43.28(88)
E4-4	71.52	32.76	--	--	45.32(87)
E4-5	57.22	27.93	--	--	44.07(86)
E4-6	47.37	25.84	--	--	48.43(76)
E4-7	52.45	26.51	--	--	50.78(80)
E4-8	51.78	25.87	--	--	47.48(87)
E4-9	57.73	27.33	--	--	46.78(85)
E4-10	67.95	28.27	--	--	51.70(83)
AVE	59.69	28.42	--	--	45.91
E5-1	--	--	91.15	--	58.36(85)
E5-2	--	--	89.42	--	65.30(82)
E5-3	--	--	90.98	--	67.45(80)
E5-4	--	--	84.62	--	82.57(71)
E5-5	--	--	86.57	--	81.10(73)
E5-6	--	--	79.94	--	77.45(71)
E5-7	--	--	92.29	--	64.93(83)
E5-8	--	--	91.12	--	60.93(84)
E5-9	--	--	88.87	--	66.96(80)
E5-10	--	--	79.87	--	61.87 (77)
AVE	--	--	87.48	--	68.69

Note: "--" denotes that there is a large deviation between the measured value and the theoretical value; "( )" in manual column denotes the gray value by manual

It can be seen that with the increase of the crystal ratio, the critical gray value needs to be reduced. For pure glass samples, the error is around 3%. As binder and pore under the microscope should be consistent to the glass in theory, we consider that this part of error is entirely due to the system error, for instance, the electronic imaging and the recognition level of the application. And for pure potassium feldspar samples, the error is between 8% and 18%. This is partly due to the system error, and partly because of the space occupied by adhesive and the inevitable gaps in the bonding process. In order to correct the error of the final data, the following adjust is made:

Set the measured value of the crystal as  $Y$ , that is, the value reflected in the table, just like,  $C_{1-x}$  and  $E_{1-x}$  all means  $Y_1$ , and the correction value is  $Y'$ . The measured value of the glass is  $X$ ,  $X=100-Y$ , and the correction value is  $X'$ . We defined the system error as  $P_0$ ,  $P_0=Y_1/100$ , it is, the proportion of crystal which the system identified in the pure glass (c1 group and e1 group) samples. The crystal's proportion of pure potassium feldspar sample was defined as  $P_{100}$ ,  $P_{100}=Y_5/100$ , means the error of the identification of the pure crystal. After the actual correction, the ratio is expressed as  $P_y$ .

We have  $P_y = Y / (X' + Y')$ .

$X / (1 - P_0)$  is the actual amorphous part, including glass, colloidal impurities and pores. Set the colloidal impurities and pores as  $X_2$ ,  $X' = X / (1 - P_0) - X_2$ . The impurities and pores content in the glass is roughly represented as them of the whole sample, so  $X_2 = X^* (1 - P_{100})$ . And we can also figure out that  $Y' = (Y - P_0 * 100) / P_{100}$ .

So we have that:  $P_y = ((Y - P_0 * 100) / P_{100}) / (X / (1 - P_0) - X^* (1 - P_{100}) + (Y - P_0 * 100) / P_{100})$

We substituted the corrected formula into the calculation, and the results are shown in the following table 3,  $P_y =$  correction value / 100.

**Table 3.** The average value after been corrected

Number	correction value of the machine cognition	correction value of the manual cognition
C1	0.00	0.00
C2	28.99	38.74
C3	56.18	57.89
C4	78.55	68.59
C5	104.32	87.88
E1	0.00	0.00
E2	39.57	29.26
E3	58.10	45.65
E4	63.74	60.92
E5	89.42	80.59

As can be seen from Table 3, after the correction, the error of machine cognition of group c is about 4-6%, the error of manual cognition of group c is about 7-13%, and the same of group e is 3-14% and 5-20%. All of them were significantly lower than before, and some of them are acceptable. Parallel comparison, we found that the accuracy of machine cognition was higher than manual cognition, and the higher the crystal content, the greater the error. Not only do we know that the gray value of the image depends on the properties of the sample itself, but also it depends on

external conditions such as the level of electronic imaging and the intensity of the light source. When the operator's level is disturbed by the above conditions, the accuracy of the result will fluctuate. But the machine recognition can approach the real value of the sample with a stable error due to the fixed parameters. Therefore, we recommend that the gray value around 70-80 can be selected for machine recognition on the whole. Under this gray value, the average error is closer to the theoretical value. Secondly, the accuracy of cognition of group c is higher than group e, indicating that the selection of adhesive has a great influence on this verification experiment.

#### 4. CONCLUSIONS

According to the above results, we draw the following conclusions:

- (1) This method of the quantitative calculation of the crystal-glass two phases is reliable.
- (2) We recommend using machine recognition with a gray value around 70-80 for quantitative calculation.
- (3) If we want to verify this method, the selection of materials and adhesives as well as the observation conditions need to be carefully prepared.

At present, digital polarizing microscope, scanning electron microscope and others are usually used to conduct electronic imaging of the rock thin section. The specific image analysis relies on their supporting accessories and software. The method is limited, and some tests are expensive. We use ImageJ, a free software designed with an open architecture, to solve almost any image processing or analysis problem. If this approach is considered feasible by peers, it is going to be an interdisciplinary innovation in the analysis of petrology, and helpful for researchers to make qualitative or quantitative judgments quickly and conveniently. The two-phase separation and quantitative calculation are only a specific attempt of ImageJ, and there will be more extensive application space to be expected.



**COMPETING INTERESTS**

No conflict of interests exists in the submission of this manuscript, and the manuscript is approved by all authors for publication.

**ACKNOWLEDGMENTS**

This work was supported by the National Science Foundation Project of China (grant Nos. 40573057 and 41673083), Open Project of the State Key Laboratory of Loess and Quaternary Geology (grant No. SKLLQG1511).

**REFERENCES**

- [1] Abramoff, M.D., Magelhaes, P.J. and Ram., S.J.: Image processing with ImageJ, *Biophotonics International*. 11, 36-42, 2004.
- [2] Bi, L., Zhang, B., and Pan, J.: Analyze soil structure characteristics by ImageJ, *Soil*. 41(4). 654-658, 2009.
- [3] Tony, j.C.: Image J for Microscopy, *BioTechniques*. 43, 25-30, 2007. [View Article](#)
- [4] <https://imagej.nih.gov/ij/docs/intro.html> [EB/OL].
- [5] <https://imagej.nih.gov/ij/docs/intro.html> [EB/OL].
- [6] Prior, D.J, Boyle, A.P, and Brenker, F.E.: The application of electron back scatter diffraction and orientation contrast imaging in the SEM to textural problems in rocks, *American Mineralogist*. 84: 1 741-1 759, 1999.
- [7] Trimby, P.W, and Prior, D.J.: Microstructural imaging techniques: A comparison between light and scanning electron microscopy, *Tectonophysics*. 303: 71-81, 1999. 00263-7 [View Article](#)
- [8] Trimby, P.W, and Prior, D.J.: Microstructural imaging techniques: A comparison between light and scanning electron microscopy, *Tectonophysics*. 303: 71-81, 1999. 00263-7 [View Article](#)
- [9] Anne, P and Ste'phanie, R.: Bioalteration of synthetic Fe(III)-, Fe(II)-bearing basaltic glasses and Fe-free glass in the presence of the heterotrophic bacteria strain *Pseudomonas aeruginosa*: Impact of siderophores, *Geochim et Cosmochim Acta*. 188 147-162, 2016. [View Article](#)
- [10] João, C.S and Neil, B.M.: The effect of the rock type on the degradation of well cements in CO2 enriched geothermal environments, *Geothermics*. 75, 235-248, 2018. [View Article](#)